

Yamamoto et al., <http://www.jcb.org/cgi/content/full/jcb.201211048/DC1>

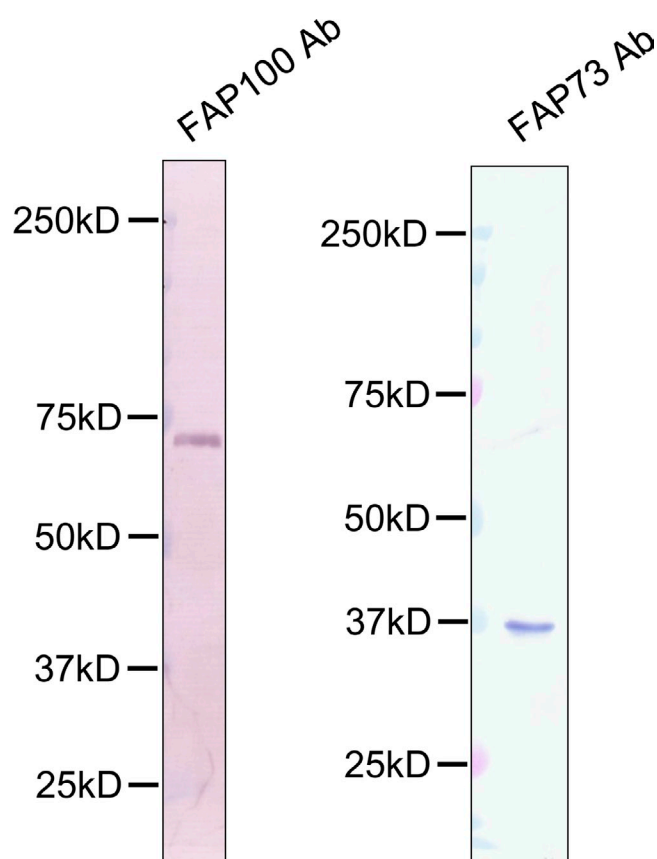
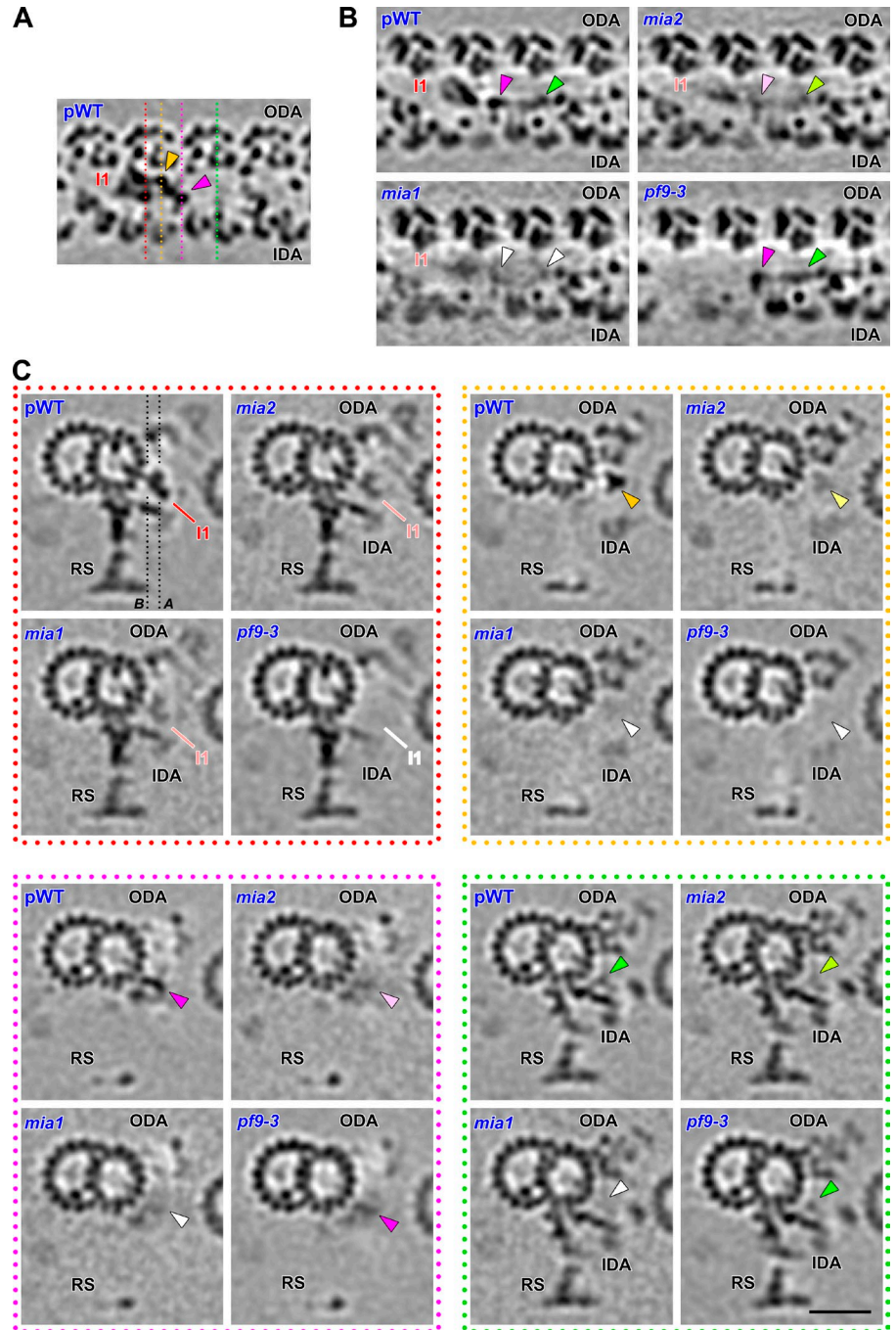


Figure S1. **The FAP100 and FAP73 antibodies are specific for the Mia1 and Mia2 proteins.** Immunoblots of wild-type axonemes were probed with the affinity-purified FAP100 and FAP73 antibodies. The FAP100 antibody detects a single band of ~70 kD, and the FAP73 antibody detects a single band of ~35 kD. The size of both bands is approximately consistent with the predicted mass for both the Mia1 and Mia2 proteins. Ab, antibody.

Figure S2. **Structural defects in *mia* mutants revealed by cryo-ET.** (A–C) Tomographic slices of the averaged 96-nm axonemal repeats from pWT, *mia2*, *mia1*, and *pf9-3/ida1*, viewed longitudinally from the front (A and B; proximal is on the left) and in cross section (C; from proximal to distal). (A) Same pWT image as shown in Fig. 6 B but with colored lines indicating the locations of the tomographic slices shown in C with the corresponding colored frames; arrowheads highlight densities that show reduction or are missing in the *mia* mutants. (B) Tomographic slices in the same orientation as A but with a cutting plane closer to the DMT; black lines in the pWT image of C (in red frame) indicate the cutting planes of A and B. Arrowheads point at regions where the densities are reduced in *mia2* (light pink and light green arrowheads) or missing/dramatically reduced in *mia1* (white arrowheads). The corresponding regions appear to be normal in both pWT and *pf9-3/ida1* (pink and green arrowheads). Note that the density of I1 dynein is reduced in both *mia* mutants and missing in *pf9-3/ida1*. (C) Cross-sectional views from four different locations along the length of the axonemal repeat show the structural defects in *mia* mutant axonemes. The distal region of the I1 IC/LC complex (yellow arrowheads) and two additional regions (pink and green arrowheads) display defects in *mia* mutant axonemes. The defects observed are more severe in *mia1* (white arrowheads) than in *mia2* (arrowheads with light colors). In *pf9-3/ida1*, the regions highlighted in red and yellow in pWT (I1 dynein) are also missing, whereas the two distal regions (pink and green arrowheads) are present at nearly wild-type level. The pWT and *pf9-3/ida1* data were refined from data originally reported by Heuser et al. (2012). Bar, 25 nm; valid for A–C.



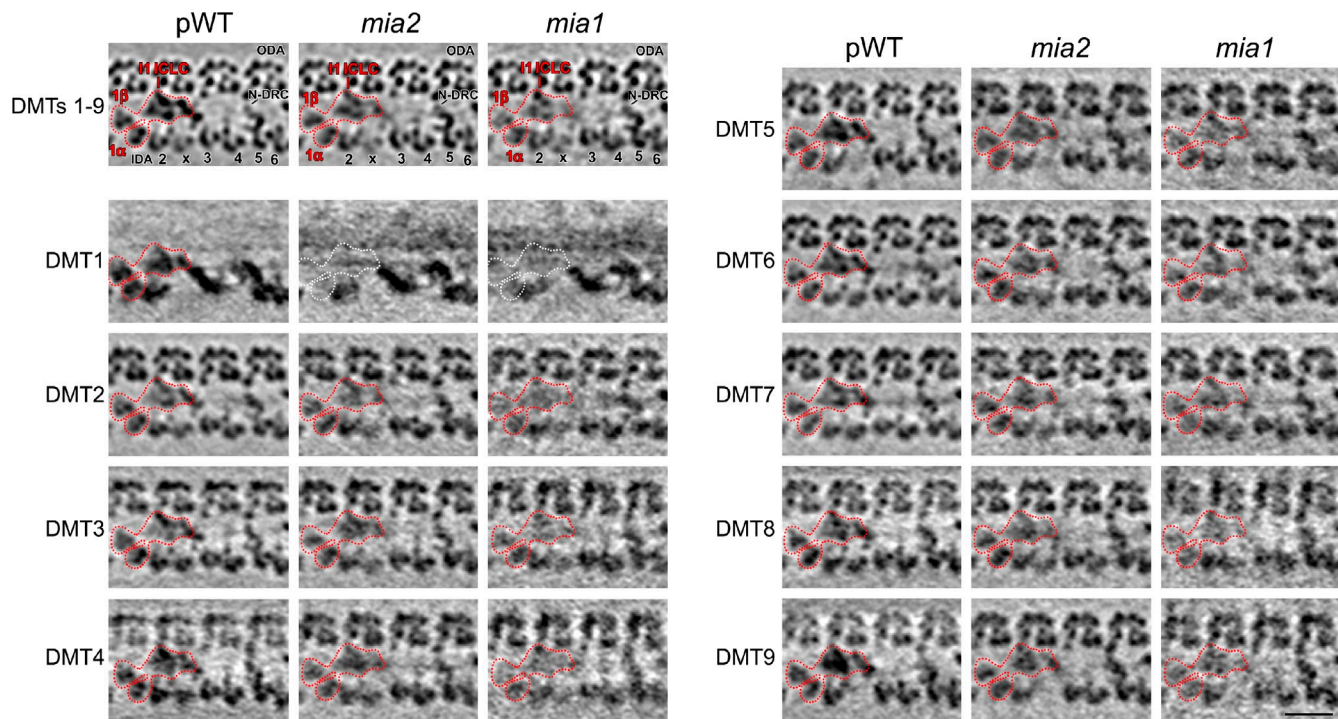


Figure S3. **I1 dynein is assembled on outer DMTs 2–9 but missing on DMT1 in the *mia* mutants.** Tomographic slices of averaged axonemal repeats from pWT, *mia2*, and *mia1*. Longitudinal front views of all doublets combined (DMTs 1–9) and of each individual doublet (DMT1 to DMT9) are shown. As shown in Fig. 7 A, the entire I1 dynein is missing or dramatically reduced on DMT1 from both *mia* mutants (white outlines). Consistent with the results of all doublets combined, the individual doublet-specific averages of DMT2 to DMT9 show a reduced density of the I1 dynein in *mia* mutants compared with pWT; this reduction appears more severe in *mia1*. The pWT data were refined from data originally reported by Heuser et al. (2009) and Lin et al. (2012). red outlines, I1 dynein complex. Bar, 25 nm.

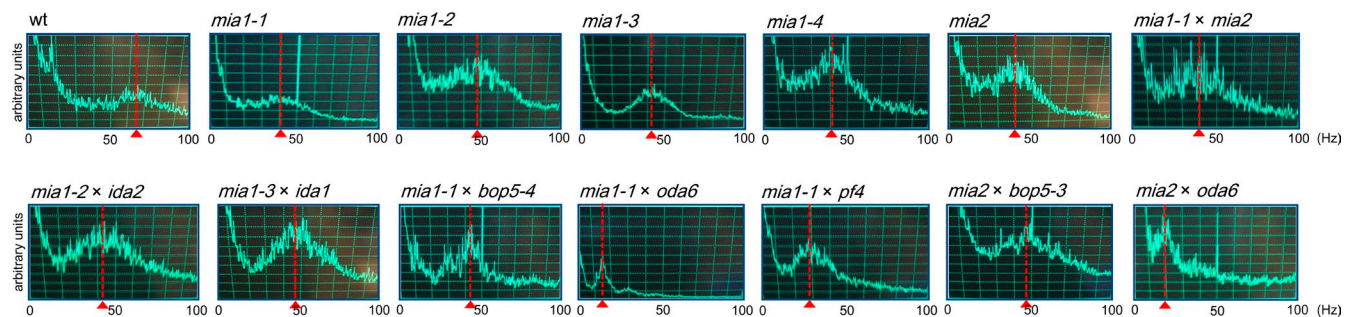


Figure S4. **The *mia* mutants have reduced beat frequencies.** Beat frequency measurements show that the *mia* mutants have reduced beat frequencies (~40–50 Hz) relative to wild type (60–70 Hz). Double mutants between the *mia* mutants and *oda6* or *pf4* have reduced beat frequencies (10–30 Hz). In contrast, doubles between the *mia* mutants and I1 dynein (*ida1*, *ida2*, *bop5-3*, and *bop5-4*) have beat frequencies similar to that of the *mia* alone (40–50 Hz). The fast Fourier transform power spectra show the approximate distribution of flagellar beat frequency and the peaks in the spectra represent the mean flagellar beat frequencies of 10–100 cells (red arrowheads and dotted lines; Kamiya, 2000). wt, wild type.

A

```

FAP100      1 -----MPIYDEASVPG--TAAGRSTTDVGAATAGANPFNIPADE
CCDC37      1 MSEIPSTIVSKNMTNDKNSLESNNISSSSSTEENPKKQAKNEEHGPDPSANPFLSGDVG
CCDC38      1 -----MSENLLPLTNSGGKVKDGSTKEDRPYKIFFR-

FAP100      37 EIFRFREERERARKEDQKLTATQTRVADKTTFAAQMOATATADARTTLR----ELRPPKG
CCDC37      61 DFFLLRDOERNKALSERQOQKTRMVHOKMTYSSKVSARKHSLRRLQLLEDKQEDLEARAE
CCDC38      32 DLFVLKENEMAAKETEFMNRNMKVYQRTTFSSRMKSHSYLSQLAFYP-----KRSGRS

FAP100      92 PKATTTLAASSVGTLDRLKEK---ENMADFIAKKREIFLLQMSLDTKRAEIKKLEERAR
CCDC37     121 AEHQRAFRDYTTWKLTLTKENVEPENMSGYTKQKROMFLLOYALDVKKREIQRLLETLAT
CCDC38      86 FEKFGPGPPIPIRLIEGSDTK---RTVHEFTNDQDRFLLEYALSTKKNITIKKFEKDIA

FAP100     148 QREFAKKKSEOMLEEDALRFDAFLKENDEKVOEATKKAEAEAKAKQDKVLEIKRINTATA
CCDC37     181 KEEARLERAEKSLKDAALDFEFVRENDCSSVQAMRAAEKETKAKIEKKLEIRDLTTQIV
CCDC38     142 MRERQLKKAEEKLQDDALAFEEFLRENDQRSVDADKMAAQETINKLQMTAEELKASMEVQ

FAP100     208 ALRSELNKKYEEQLEDCCRYYKEFLDSITPPEWFEQQAQ---LQRRKDALVAEWSQCEAL
CCDC37     241 NIKSEISRFEDTLKHVKYKDFLYKLSPKKEWLEEQEKKHSEFLKKAKEVSEASKESVNST
CCDC38     202 AVKSEIAKTEFLLREYMKYGFLLQMSPKHWQIQQALKRAQASKSANIILPKILAKLSL

FAP100     265 KQREAAALAAKTAESDYAN-----ARTQQAERAERAIKESVAAALKBIM
CCDC37     301 PGDKGPGTKGKASSMWAKEGQGTKKPWRFLQTMRLQRSPSYLSSPQGGSQPSESSEGGDSF
CCDC38     262 HSSNKEGLEESGRTAVLSEDAEQGR-----DSQKPSRSLTRTPKKKKNLAESEF

FAP100     310 KEKEPQPP-NLDFEMDPEDDEMYFOEPFGOLLAVYKOLEESNLFYIQNAQETEEALEELRQ
CCDC37     361 GSNSEPIPTQEDTDSDEEPQLYFTEPQQLLDVFRELEEQNLSLIQNSQETEKLEELSH
CCDC38     313 GSEDSLEFLLDDEMDVDLEPALYFKEPEELLQVLRLEEQNLTLFQYSQVDENLEEVNK

FAP100     369 KLRDTKTRMDAEAGLQGVSTTQASIVAAREKAKRLKDRTLNENGAFTLSMGGSSNAPTS
CCDC37     421 TLKHTQIRMDREVNQLKQWVTMMMSITKEEDTAAELELKA-----VFHFG-----
CCDC38     373 REKVIQDKTNSNIEFLLQEKMKKANCVREEKAELQLKSK-----TFSFG-----

FAP100     429 SVTGSSGPGGPVNNKELGDKVREVVYVRCG-FDADASISTQMLTNIEMKLEEYLNLAEGM
CCDC37     468 ---EYKGDQDKLLESNLCKVLDVYRHCTGTQQEANTGTVOMLTIEHQLELLENLHV
CCDC38     420 ---EFNSDAQEILLDSLSKKITQVYKVCIGDAEDDGLNPIQKLVKVESRLVELCDLIESI

FAP100     488 TPDYVDGAEKAREKDRRKVARDEKLSTOHREHEARMARALERAAAPVFKTKGKPLMFRSA
CCDC37     525 PQVKIEQAEARAKERKRIRLREKQLQMKILQEEHQRARARAQAEIKKKRGRLVCRSR
CCDC38     477 PKENVEAIERMKQKEWRQKFRDEKMKKQRHQQERLKAALBKAVAPQKKLGRRLVFSK

FAP100     548 PPQRKKVVQADDRNDEEALELAYLAQDMI
CCDC37     585 PPAHRKIQQSEHTLMDKBEELFFFT--
CCDC38     537 PPSGNKQQLPLVNETKTKSQEERYFFT--

```

B

```

CCDC42A      1 MSLGIMEEEDLAEYFRLQYGERLLQMLQKLPNVEGASESPSIWLLKKKSTEIMHQTMOVQ
CCDC42B      1 -----MAVPWEYFRLALQEKLS---TKLPEQAEDHVPVLRLLLEKROELVDADQALQA
FAP73        1 -----MDEEGSATARAKMMP-----QTLVLVHVSPATRLLEKRRQMFVEQEALEA

CCDC42A      61 KKKMFORMETLNLRWELGVKEAQLKAHIQKSEOFHOENDQKRTAMKKANKERELKCO
CCDC42B      52 QREVFRTKTAALKORWEQLEQERELKGSFIRFDKFLQDSERRNRALRAAERHQAGR
FAP73        46 QKQDFNRKEEVFKRREBALKLKDLELQESLIRFSKFLQENDSKRRAEKKANDETKARIQ

CCDC42A     121 HMQELTKRKQEMVALRLEHORLSAKLKYDYIFNKYLEKVVENSE-FEETHEVIARYKTLV
CCDC42B     112 REVEALRLWTQLQELRREHARLQRRLLKRLPCARLLQALELPLPGFQEVPELVAREFDGLA
FAP73       106 KEKEIEQLTEVLEELKSEKERILEVLEKNMRYQHYLESVLEVADEYQEVADLLRHATLS

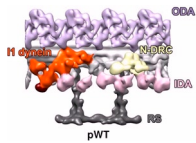
CCDC42A     180 SMRHDLMQSAQEGQEKIERAKARLARYMEEKDDEILOQNNELARLQMRFRDRARSNVIFWE
CCDC42B     172 ETQAAELRLREREQLAELEAARALQQLRDAPDEVLAQGGORRAQLQERLEAARERTLOWE
FAP73       166 ATNADLKDHQKCSLAEKVRTELEQIVYKQKDEILNLNNQVAKLKTELEGYEAEAMVQE

CCDC42A     240 SEWAHIQNTAAKKTLLLTGTIKMATLNLFOIVSKHLKEVTEVALEDTHKQOLDMIQOQFIQDR
CCDC42B     232 SKWIOIQNTAAEKTLLLGRSRMAVLNLFOLVCOHQGPPTLDIEDTEGQLEHVLFMDQL
FAP73       226 AKKDSLSQIASQRTLEYQVVLSDADNIFN-RCRSKSSIGHPEESNPLHQLDVIGNFVSDL

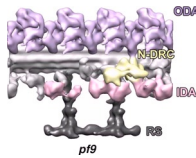
CCDC42A     300 SDIWAEEVKKKEQQQVRI-----
CCDC42B     292 SAMLAGLGQAEPAAPAS-----
FAP73       285 GSTIKQFKQEQAKRASLASRAEIE

```

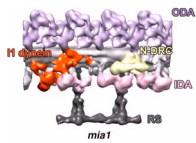
Figure S5. **Sequence comparisons of *C. reinhardtii* Mia proteins with their potential human homologues.** (A) Sequences of *C. reinhardtii* FAP100 and two potential human homologues, CCDC37 and CCDC38, were aligned using ClustalW, and the output was processed with BoxShade. Characters with black and gray backgrounds represent identical and similar amino acids, respectively. Accession numbers are as follows: *C. reinhardtii* FAP100, AB692780; *Homo sapiens* CCDC37, AAI01369; and *Homo sapiens* CCDC38, AAH95479. (B) Sequences of *Chlamydomonas reinhardtii* FAP73 and two potential human homologues, CCDC42A and CCDC42B, were aligned as described for A. Accession numbers are as follows: *C. reinhardtii* FAP73, AB692781; *Homo sapiens* CCDC42A, Q96M95; and *Homo sapiens* CCDC42B, NP_001138344. Accession numbers were obtained from the NCBI protein and NCBI nucleotide databases.



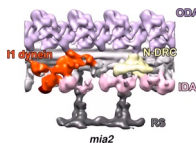
Video 1. **3D visualization of pWT axonemes.** Shown is an animated 3D isosurface rendering of the averaged 96-nm axonemal repeat from pWT *C. reinhardtii* flagella. At the beginning of the video, the proximal end of the repeat is on the left side. Labels and coloring: I1 dynein (orange), I1 tether head (red), nexin-dynein regulatory complex (N-DRC; yellow), inner dynein arms (IDAs; rose), outer dynein arms (ODAs; purple), and radial spokes (RSs; dark gray).



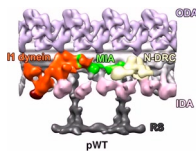
Video 2. **3D visualization of pf9-3/ida1 axonemes.** Shown is an animated 3D isosurface rendering of the averaged 96-nm axonemal repeat from pf9-3/ida1 *C. reinhardtii* flagella. Note that the entire I1 dynein complex is missing. At the beginning of the video, the proximal end of the repeat is on the left side. Labels and coloring: nexin-dynein regulatory complex (N-DRC; yellow), inner dynein arms (IDAs; rose), outer dynein arms (ODAs; purple), and radial spokes (RSs; dark gray).



Video 3. **3D visualization of mia1 axonemes.** Shown is an animated 3D isosurface rendering of the averaged 96-nm axonemal repeat from mia1 *C. reinhardtii* flagella. Note that the distal density of the I1 dynein complex and the density between the I1 dynein and the N-DRC are significantly reduced. At the beginning of the video, the proximal end of the repeat is on the left side. Labels and coloring: I1 dynein (orange), I1 tether head (red), nexin-dynein regulatory complex (N-DRC; yellow), inner dynein arms (IDAs; rose), outer dynein arms (ODAs; purple), and radial spokes (RSs; dark gray).



Video 4. **3D visualization of mia2 axonemes.** Shown is an animated 3D isosurface rendering of the averaged 96-nm axonemal repeat from mia2 *C. reinhardtii* flagella. Note that the distal density of the I1 dynein complex is reduced. At the beginning of the video, the proximal end of the repeat is on the left side. Labels and coloring: I1 dynein (orange), I1 tether head (red), nexin-dynein regulatory complex (N-DRC; yellow), inner dynein arms (IDAs; rose), outer dynein arms (ODAs; purple), and radial spokes (RSs; dark gray).



Video 5. **3D localization of the MIA complex.** Based on a pWT-mutant comparison, the axonemal structures affected in the mia mutants are colored in green in the animated 3D isosurface rendering of the averaged 96-nm axonemal repeat from pWT *C. reinhardtii* flagella. At the beginning of the video, the proximal end of the repeat is on the left side. Labels and coloring: I1 dynein (orange), I1 tether head (red), MIA complex and associated structures (green), nexin-dynein regulatory complex (N-DRC; yellow), inner dynein arms (IDAs; rose), outer dynein arms (ODAs; purple), and radial spokes (RSs; dark gray). Compare with Fig. 6 C.

Table S1. Potential MIA complex components identified by chemical cross-linking and immunoprecipitation

Protein number	Protein definition	Score
FAP100-HA		
GI 159477649 ^a	Flagellar inner dynein arm I1 IC, IC138	137
GI 159471389	Flagellar-associated protein, FAP189	48
GI 159486503	Flagellar-associated protein, FAP57	46
GI 30580462 ^a	Dynein-1- β HC, flagellar inner arm I1 complex	41
GI 159463370	Flagellar-associated protein, FAP68	35
GI 159485950	Flagellar/basal body protein, FBB10	35
GI 30580468 ^a	Dynein-1- α HC, flagellar inner arm I1 complex	33
GI 159489898	SWI/SNF chromatin-remodeling complex component	30
GI 159472759	Predicted protein	26
GI 159483703	Flagellar/basal body protein, PACRG-like protein	25
GI 159467413	DNA-directed RNA polymerase II, largest subunit	25
GI 1354832	RpoC2 protein, partial (chloroplast)	23
GI 159471658	Predicted protein, partial	23
GI 159474306	Flagellar-associated protein, FAP44	20
FAP73-HA		
GI 30580462 ^a	Dynein-1- β HC, flagellar inner arm I1 complex	107
GI 159474916	RWP-RK transcription factor	31
GI 159489926	5-enolpyruvylshikimate-3-phosphate synthase	26
GI 159485936	Hypothetical protein CHLREDRAFT_167801	25
GI 159477649 ^a	Flagellar IDA I1 IC, IC138	24
GI 159483705	Hypothetical protein CHLREDRAFT_141667, partial	24
GI 159472228	Hypothetical protein CHLREDRAFT_196913	24
GI 159483703	Flagellar/basal body protein, PACRG-like protein	23
GI 159481544	Flagellar-associated protein, FAP43	23
GI 159468520	Predicted protein	23
GI 159481574	Hypothetical protein CHLREDRAFT_151956, partial	22
GI 159481750	Hypothetical protein CHLREDRAFT_152015, partial	21
GI 159481859	T-type cyclin	21
GI 159478731	Predicted protein, partial	21
GI 159480608	Predicted protein	20

Protein number shows the gene index (GI) number of the protein in NCBI Protein database. Protein definition is the definition of the protein in NCBI. Score shows MASCOT probability score of ESI/liquid chromatography /MS/MS analysis. SWI/SNF, switch/sucrose nonfermentable.

^aPreviously identified I1 dynein components.

Table S2. Mutant strains used in this study

Mutant	Affected protein	Axonemal defect	Reference
137c (wild type)	N/A	None	Harris, 1989
pWT (<i>pf2-4::PF2-GFP</i>) ^a	N/A	None	Rupp and Porter, 2003; Heuser et al., 2009
<i>bop5</i>	IC138	Loss of I1 dynein regulatory subcomplex	Hendrickson et al., 2004; VanderWaal et al., 2011
<i>ida1/pf9</i>	DHC1	Loss of I1 dynein	Kamiya et al., 1991; Myster et al., 1997
<i>ida2</i>	DHC10	Loss of I1 dynein	Kamiya et al., 1991; Perrone et al., 2000
<i>ida3</i>	Unknown	Loss of I1 dynein	Kamiya et al., 1991
<i>ida4</i>	p28	Loss of dynein a, c, and d	Kamiya et al., 1991; LeDizet and Piperno, 1995
<i>ida5</i>	Actin	Loss of dynein a, c, d, and e	Kato-Minoura et al., 1997
<i>ida6</i>	Unknown	Loss of dynein e; defect in N-DRC	Kato et al., 1993; Porter, 2011
<i>ida9</i>	DHC9	Loss of dynein c	Yagi et al., 2005
<i>mia1-1</i>	FAP100	Defect in the MIA complex	King and Dutcher, 1997; this study
<i>mia1-2</i>			
<i>mia1-3</i>			
<i>mia1-4</i>			
<i>mia2</i>	FAP73	Defect in the MIA complex	King and Dutcher, 1997; this study
<i>mbo1</i>	Unknown	Loss of beaklike structure	Segal et al., 1984
<i>mbo2</i>	Mbo2p	Loss of beaklike structure	Segal et al., 1984; Tam and Lefebvre, 2002
<i>oda1</i>	DC2	Loss of ODA	Kamiya, 1988; Takada et al., 2002
<i>oda2</i>	DHC15	Loss of ODA	Kamiya, 1988; Wilkerson et al., 1994
<i>oda6</i>	IC2	Loss of ODA	Kamiya, 1988; Mitchell and Kang, 1991
<i>oda7</i>	Oda7p	Loss of ODA	Kamiya, 1988; Freshour et al., 2007
<i>pf3</i>	DRC1	Loss of dynein e; defect in N-DRC	Piperno et al., 1992, 1994; Gardner et al., 1994
<i>pf4</i>	PP2A	Loss of protein phosphatase 2A B subunit	Elam et al., 2011
<i>pf14</i>	RSP3	Loss of RSs	Luck et al., 1977
<i>pf17</i>	RSP9	Loss of RS heads	Harris, 1989; Yang et al., 2006
<i>pf18</i>	Unknown	Loss of CP	Harris, 1989

N/A, not applicable.

^aThe pseudo-wild-type strain (pWT) is a rescued mutant that is biochemically, structurally, and phenotypically indistinguishable from wild type. It was generated by transforming the N-DRC mutant *pf2* with a GFP-tagged *PF2* gene from wild type.

Table S3. Resolution of 3D structures obtained by cryo-ET

Mutant name	Strain	Averaged repeats	Resolution		
			DMT	ODA	I1 dynein
pWT ^a	<i>pf2-4::PF2-GFP</i>	720	<i>nm</i>	<i>nm</i>	<i>nm</i>
<i>mia1</i>	<i>mia1-1</i>	750	3.1	3.5	3.3
<i>mia2</i>	<i>mia2</i>	1,200	3.8	4.1	4.3
<i>pf9/ida1</i> ^b	<i>pf9-3</i>	1,100	3.5	3.5	4.3
			3.2	3.7	—

Resolution (0.5 Fourier shell correlation criterion) was measured at two different locations: the DMT usually has the highest resolution in the axonemal averages; the I1 dynein has usually a slightly lower resolution, which is typical for associated complexes. The minus sign indicates that I1 dynein is absent.

^aData were used as control and were refined from data originally published by Heuser et al. (2009) and Lin et al. (2012).

^bData were used as control and were refined from data originally published by Nicastro et al. (2006) and Heuser et al. (2012).

References

- Elam, C.A., M. Wirschell, R. Yamamoto, L.A. Fox, K. York, R. Kamiya, S.K. Dutcher, and W.S. Sale. 2011. An axonemal PP2A B-subunit is required for PP2A localization and flagellar motility. *Cytoskeleton (Hoboken)*. 68:363–372. <http://dx.doi.org/10.1002/cm.20519>
- Freshour, J., R. Yokoyama, and D.R. Mitchell. 2007. *Chlamydomonas* flagellar outer row dynein assembly protein ODA7 interacts with both outer row and I1 inner row dyneins. *J. Biol. Chem.* 282:5404–5412. <http://dx.doi.org/10.1074/jbc.M607509200>
- Gardner, L.C., E. O'Toole, C.A. Perrone, T. Giddings, and M.E. Porter. 1994. Components of a “dynein regulatory complex” are located at the junction between the radial spokes and the dynein arms in *Chlamydomonas* flagella. *J. Cell Biol.* 127:1311–1325. <http://dx.doi.org/10.1083/jcb.127.5.1311>
- Harris, E.H. 1989. The *Chlamydomonas* Sourcebook: A Comprehensive Guide to Biology and Laboratory Use. Academic Press, San Diego, CA. 780 pp.
- Hendrickson, T.W., C.A. Perrone, P. Griffin, K. Wuichet, J. Mueller, P. Yang, M.E. Porter, and W.S. Sale. 2004. IC138 is a WD-repeat dynein intermediate chain required for light chain assembly and regulation of flagellar bending. *Mol. Biol. Cell.* 15:5431–5442. <http://dx.doi.org/10.1091/mbc.E04-08-0694>
- Heuser, T., M. Raytchev, J. Krell, M.E. Porter, and D. Nicastro. 2009. The dynein regulatory complex is the nexin link and a major regulatory node in cilia and flagella. *J. Cell Biol.* 187:921–933. <http://dx.doi.org/10.1083/jcb.200908067>
- Heuser, T., C.F. Barber, J. Lin, J. Krell, M. Rebesco, M.E. Porter, and D. Nicastro. 2012. Cryoelectron tomography reveals doublet-specific structures and unique interactions in the I1 dynein. *Proc. Natl. Acad. Sci. USA.* 109:E2067–E2076. <http://dx.doi.org/10.1073/pnas.1120690109>
- Kamiya, R. 1988. Mutations at twelve independent loci result in absence of outer dynein arms in *Chlamydomonas reinhardtii*. *J. Cell Biol.* 107:2253–2258. <http://dx.doi.org/10.1083/jcb.107.6.2253>
- Kamiya, R. 2000. Analysis of cell vibration for assessing axonemal motility in *Chlamydomonas*. *Methods.* 22:383–387. <http://dx.doi.org/10.1006/meth.2000.1090>
- Kamiya, R., E. Kurimoto, and E. Muto. 1991. Two types of *Chlamydomonas* flagellar mutants missing different components of inner-arm dynein. *J. Cell Biol.* 112:441–447. <http://dx.doi.org/10.1083/jcb.112.3.441>
- Kato, T., O. Kagami, T. Yagi, and R. Kamiya. 1993. Isolation of two species of *Chlamydomonas reinhardtii* flagellar mutants, *ida5* and *ida6*, that lack a newly identified heavy chain of the inner dynein arm. *Cell Struct. Funct.* 18:371–377. <http://dx.doi.org/10.1247/csf.18.371>
- Kato-Minoura, T., M. Hirono, and R. Kamiya. 1997. *Chlamydomonas* inner-arm dynein mutant, *ida5*, has a mutation in an actin-encoding gene. *J. Cell Biol.* 137:649–656. <http://dx.doi.org/10.1083/jcb.137.3.649>
- King, S.J., and S.K. Dutcher. 1997. Phosphoregulation of an inner dynein arm complex in *Chlamydomonas reinhardtii* is altered in phototactic mutant strains. *J. Cell Biol.* 136:177–191. <http://dx.doi.org/10.1083/jcb.136.1.177>
- LeDizet, M., and G. Piperno. 1995. *ida4-1*, *ida4-2*, and *ida4-3* are intron splicing mutations affecting the locus encoding p28, a light chain of *Chlamydomonas* axonemal inner dynein arms. *Mol. Biol. Cell.* 6:713–723.
- Lin, J., T. Heuser, K. Song, X. Fu, and D. Nicastro. 2012. One of the nine doublet microtubules of eukaryotic flagella exhibits unique and partially conserved structures. *PLoS ONE.* 7:e46494. <http://dx.doi.org/10.1371/journal.pone.0046494>
- Luck, D., G. Piperno, Z. Ramanis, and B. Huang. 1977. Flagellar mutants of *Chlamydomonas*: studies of radial spoke-defective strains by dikaryon and revertant analysis. *Proc. Natl. Acad. Sci. USA.* 74:3456–3460. <http://dx.doi.org/10.1073/pnas.74.8.3456>
- Mitchell, D.R., and Y. Kang. 1991. Identification of *oda6* as a *Chlamydomonas* dynein mutant by rescue with the wild-type gene. *J. Cell Biol.* 113:835–842. <http://dx.doi.org/10.1083/jcb.113.4.835>
- Myster, S.H., J.A. Knott, E. O'Toole, and M.E. Porter. 1997. The *Chlamydomonas* Dhc1 gene encodes a dynein heavy chain subunit required for assembly of the I1 inner arm complex. *Mol. Biol. Cell.* 8:607–620.
- Nicastro, D., C. Schwartz, J. Pierson, R. Gaudette, M.E. Porter, and J.R. McIntosh. 2006. The molecular architecture of axonemes revealed by cryoelectron tomography. *Science.* 313:944–948. <http://dx.doi.org/10.1126/science.1128618>
- Perrone, C.A., S.H. Myster, R. Bower, E.T. O'Toole, and M.E. Porter. 2000. Insights into the structural organization of the I1 inner arm dynein from a domain analysis of the Ibeta dynein heavy chain. *Mol. Biol. Cell.* 11:2297–2313.
- Piperno, G., K. Mead, and W. Shestak. 1992. The inner dynein arms I2 interact with a “dynein regulatory complex” in *Chlamydomonas* flagella. *J. Cell Biol.* 118:1455–1463. <http://dx.doi.org/10.1083/jcb.118.6.1455>
- Piperno, G., K. Mead, M. LeDizet, and A. Moscatelli. 1994. Mutations in the “dynein regulatory complex” alter the ATP-insensitive binding sites for inner arm dyneins in *Chlamydomonas* axonemes. *J. Cell Biol.* 125:1109–1117. <http://dx.doi.org/10.1083/jcb.125.5.1109>
- Porter, M.E. 2011. Flagellar motility and the dynein regulatory complex. In *Dyneins: Structure, Biology and Disease*. S.M. King, editor. Academic Press, Amsterdam/Boston. 337–365.
- Rupp, G., and M.E. Porter. 2003. A subunit of the dynein regulatory complex in *Chlamydomonas* is a homologue of a growth arrest-specific gene product. *J. Cell Biol.* 162:47–57. <http://dx.doi.org/10.1083/jcb.200303019>
- Segal, R.A., B. Huang, Z. Ramanis, and D.J. Luck. 1984. Mutant strains of *Chlamydomonas reinhardtii* that move backwards only. *J. Cell Biol.* 98:2026–2034. <http://dx.doi.org/10.1083/jcb.98.6.2026>
- Takada, S., C.G. Wilkerson, K. Wakabayashi, R. Kamiya, and G.B. Witman. 2002. The outer dynein arm-docking complex: composition and characterization of a subunit (*oda1*) necessary for outer arm assembly. *Mol. Biol. Cell.* 13:1015–1029. <http://dx.doi.org/10.1091/mbc.01-04-0201>
- Tam, L.W., and P.A. Lefebvre. 2002. The *Chlamydomonas* MBO2 locus encodes a conserved coiled-coil protein important for flagellar waveform conversion. *Cell Motil. Cytoskeleton.* 51:197–212. <http://dx.doi.org/10.1002/cm.10023>
- VanderWaal, K.E., R. Yamamoto, K. Wakabayashi, L. Fox, R. Kamiya, S.K. Dutcher, P.V. Bayly, W.S. Sale, and M.E. Porter. 2011. bop5 mutations reveal new roles for the IC138 phosphoprotein in the regulation of flagellar motility and asymmetric waveforms. *Mol. Biol. Cell.* 22:2862–2874. <http://dx.doi.org/10.1091/mbc.E11-03-0270>
- Wilkerson, C.G., S.M. King, and G.B. Witman. 1994. Molecular analysis of the gamma heavy chain of *Chlamydomonas* flagellar outer-arm dynein. *J. Cell Sci.* 107:497–506.
- Yagi, T., I. Minoura, A. Fujiwara, R. Saito, T. Yasunaga, M. Hirono, and R. Kamiya. 2005. An axonemal dynein particularly important for flagellar movement at high viscosity. Implications from a new *Chlamydomonas* mutant deficient in the dynein heavy chain gene DHC9. *J. Biol. Chem.* 280:41412–41420. <http://dx.doi.org/10.1074/jbc.M509072200>
- Yang, P., D.R. Diener, C. Yang, T. Kohno, G.J. Pazour, J.M. Dienes, N.S. Agrin, S.M. King, W.S. Sale, R. Kamiya, et al. 2006. Radial spoke proteins of *Chlamydomonas* flagella. *J. Cell Sci.* 119:1165–1174. <http://dx.doi.org/10.1242/jcs.02811>